Numerical Methods in Civil Engineering, 7-3 (2023) 26-44

Numerical Methods in Civil Engineering

Journal Homepage: https://nmce.kntu.ac.ir/

Identification of Critical Members in the Progressive Collapse Analysis of Two-Layer Tensegrity Barrel Vaults

Elham. Ghandi* and Vahid. Habibi Sheykh Ahmad**

ARTICLE INFO

RESEARCH PAPER

Article history:
Received:
March 2022.
Revised:
July 2022.
Accepted:
July 2022.

Keywords:
Tensegrity barrel-vault,
Finite element,
Progressive collapse,
Critical members,
Non-linear dynamic analysis

Abstract:

Tensegrity structures have a high degree of indeterminacy. The occurrence of initial partial failure at one point of these structures can lead to the propagation of failure throughout the structure. One of the influential factors in the propagation of initial failure is the initial starting point of failure. The first failure can occur in a member that is considered "critical member" and causes further damage to the structure, or it can occur in a member that has caused minor damage to the structure and maintained the overall stability of the structure. Identification of critical members in tensegrity barrel-vaults, due to the application of these structures in the roof covering of meeting halls, passenger terminals, industrial halls, aircraft hangars, etc., can lead to important and effective results in preventing the occurrence of progressive collapse and possible damages. Therefore, in this paper, the critical members of a two-layer tensegrity barrel-vaults consisting of square simplexes are identified by performing nonlinear dynamic analysis using Abaqus software. Abaqus software uses the Model Change settings to simulate the initial failure. The stability of the structure under the dynamic effects of failure of different members is investigated, and finally, the critical and non-critical members are introduced. It was found that the failure of members of the modules, which are closer to the center of the structure in the longitudinal direction of the barrel vault, shows more critical behavior than the members of other modules. Also, as observed in the results of analysis, members with maximum stress are not among the most critical members.

1. Introduction

The term tensegrity was created by Richard Buckminster Fuller as a contraction of ‘tensional’ and ‘integrity’. It refers to the integrity of a stable structure balanced by continuous structural members (cables) in tension and discontinuous structural members (struts) in compression. Moreover, the cables are flexible and global components, while the struts are stiff and local components [1]. According to Zhang and Ohsaki [1], tensegrity structures consist of two types of members which are struts to withstand pressure and cables to withstand tension. The structure is composed of straight members and it is stable without any support. The tensegrity structures are applicable in a variety of applications, including grids, barrel vaults, domes, bridges, masts, etc. The tensegrity grids are reticulated by a skeletal texture. These structures are usually interconnected by a large number of straight and sometimes curved members. If the tensegrity grids are curved around one of the longitudinal directions, the barrel vault tensegrity is formed. However, if the tensegrity grids are curved in two longitudinal directions, the tensegrity domes take shape. Tensegrity structures are usually made of units called modules. Each type of tensegrity module consists of a different number of members and has a specific shape. However, all modules, by definition, have all the necessary conditions to form tensegrity structures. Tensegrity structures consist of cable and pipe sections. Due to the small cross-sectional area of the members, the tensegrity structures are lighter than other

** Corresponding author: Associate Professor, Faculty of Technical and Engineering, University of Mohaghegh Ardabili, Ardabil, Iran. Email:ghandi@uma.ac.ir*

*** Master Graduate, Faculty of Technical and Engineering, University of Mohaghegh Ardabili, Ardabil, Iran.*

https://doi.org/10.52547/NMCE.2022.403

structures with similar applications. This feature of tensegrity structures has made them one of the suitable options for covering roofs in relatively large spans.

Tensegrity systems are mainly statically and kinematically indeterminate systems. They typically contain a large number of members, and possess a high degree of static indeterminacy. The stability analysis performed on these systems has indicated that buckling of a strut (or set of struts) or rupture of a cable may cause a progressive collapse to occur, despite high redundancy [2, 3]. Progressive collapse is the spread of initial local failure from a structural element, which eventually results in the collapse of an entire structure or a large part of it [4].

Tensegrity systems typically contain a large number of members, by the loss of any of them likely to produce serious strength reductions. When a member is lost suddenly in a tensegrity system, the energy stored in the system is released, and this induces a state of transient vibration about the new equilibrium position. Therefore, the members of the system will experience transient forces and displacements greater than the values derived from static analysis. Consequently, there is the possibility that these dynamic forces cause buckling of a strut or rupture of a cable. Failure of a second member will cause further vibration resulting in the progressive collapse of other members before a new equilibrium state is reached. Hence, it is important to account for the dynamic effects caused by the member loss in the evaluation of the response of these systems. In practice, members of a tensegrity system may be lost due to a poor member node connection. In fact, one or more faulty connections in a structure, including hundreds of connections, is a realistic possibility. The existence of geometric imperfections (e.g., lack of fit) may cause this to occur prematurely under a small portion of the total design load. In such cases, it can be argued that this member has been lost, in effect [5].

Generally, progressive collapse lasts for a short duration. Therefore, it is impossible to prevent progressive collapse in a structure once it occurs. This issue enhances the importance of understanding the response of the structure during member loss. One of the most effective methods, to assess the vulnerability of a structure to progressive collapse, is the alternate path analysis method. In this method, the defected structure is analyzed at a specified load level (e.g., design load level) to investigate the performance of the structure under distributed loads due to member loss. Then, in order to avoid the propagation of local collapse, the structure is designed in a way to sustain local collapse (i.e., member loss) and produce a new path to transmit the loads [6].

Limited studies have been conducted the progressive failure of space structures in the last decade. Shekastehband et al. [7] investigated the sensitivity of tensegrity grids to removing a member. Their analyses are performed using two methods of static and dynamic non-linear alternative paths. In conclusion, the compression members of the tensegrity grids are proposed as the critical members of the structure. Shekastehband and Abedi [8] presented a numerical and experimental investigation into the collapse behavior of tensegrity systems due to a cable rupture. It was found that the most important factors, influencing the collapse behavior of the tensegrity systems due to a cable rupture, are the damping ratios and load level at which a cable element is suddenly ruptured. Shekastehband et al. conducted experimental and numerical studies to evaluate the collapse behavior of tensegrity grids due to buckling of a strut at a critical load level [9], cable rupture, and strut collapse with snap-through [10].It was found that the most important factors that influence the collapse behavior of the tensegrity model are the imperfection amplitude, damping factors, residual stresses of the buckled struts, and the fastener bolt failure after buckling the struts. Al Sabouni-Zawadzka and Gilewski [11] studied the control of tensegrity plate due to member Loss. They have been focused on actively controlled tesegrity plates and their self-repair, considering possible damage scenarios. It has been proved that self-repair of structures, like the tensegrity plate in this research, is possible using only self-stress and does not require any external interference. Shekastehband [12] has investigated collapse mechanisms of single curvature tensegrity systems by carrying out non-linear collapse analysis using the finite element method. In his paper, six collapse mechanisms were determined as (1) Local collapse due to slackening of cables; (2) Overall collapse; (3) Local collapse with dynamic snap-through; (4) Combination of slackening of the first set of cables and local collapse with dynamic snap-through; (5) Local collapse without dynamic snap-through; (6) Local collapse with dynamic snap-through which is followed by rupture of cables. Assessment of the progressive collapse resistance of double-layer grid space structures using implicit and explicit methods has been done by Fu and Park [13]. In their study different removal scenarios were appraised notably the removal of internal central members and also support members. Though the explicit method can simulate the whole collapse process, the implicit codified method is simple and straightforward. Therefore, it can be recommended for practical engineers to use. Sychterz and Smith used dynamic measurements to detect and locate ruptured cables on a tensegrity structure [14]. In their paper, the detection and location of a ruptured cable in a deployable tensegrity footbridge are studied through monitoring changes in dynamic behavior. Non-linear dynamic instability behavior of tensegrity grids subjected to impulsive loads has been investigated by Shekastehband and Ayoubi [15]. In their paper, two geometrically rigid configurations assembled from half-cuboctahedron (HC) modules and crystal-cell pyramid (CP) modules under impulsive loads are analyzed, to compare critical dynamic loads to critical static loads. Shen et al. [16] presented a method to identify the critical members in a single-layer latticed dome. An index is proposed to evaluate the relative criticality of each dome member, which considers the influence of the load on the node, the stiffness of the connecting members, the boundary condition of the connecting members, and the angle of the gap created by the member removal. Habibi and Ghandi [17] investigate the progressive failure of double-layer tensegrity barrel vaults consisting of square simplexes using the finite element method. The analyses in this research have been performed by non-linear static and dynamic methods. The studied structures are more vulnerable to initial failure in compression members than other members. Mirzaaghazadeh et al. [18] investigated the collapse behavior of a family of tensegrity structures, i.e. di-pyramid (DP) barrel vaults that can offer promising solutions for civil engineering applications. They discussed the effects of geometric parameters, self-stress properties, loading type, boundary conditions, and strengthening schemes on the structural behavior. Significant gains in collapse resistance of these structures under symmetric loading are obtained with strengthened critical struts or cables, depending on which collapse case dominates, but the initial stiffness is not generally influenced by these schemes. Ben Kahla et al. [19] presented a non-linear dynamic analysis procedure for the investigation of the response of a tensegrity bridge to a selected sudden cable rupture. The non-linear equation of motion of the tensegrity bridge subjected to dynamic loads is discretized and integrated in time using the unconditionally stable Newmark constant-average acceleration method combined with a Newton-Raphson iterative scheme. Wu et al. [20] investigated the effect of the rupture of cables on two periodic tensegrity grids (with and without clustered cables) using the corotational approach. The results of the numerical simulation show that clustered cables play important roles in sharing external loads in a way that the clustered tensegrity grid has a uniform deformation in comparison with the classical one.

Previous studies focused more on progressive failure. However, none of the researchers analyzed all the members of the structure under study to investigate the progressive failure. In most previous studies, members with maximum stress were referred to the "critical members". Critical members refer to the members that the stability of the structure is in a more critical condition in the event of an initial failure in them. None of the studies that have been done on double-layer tensegrity barrel vaults have identified and investigated the critical members. In contrast, tensegrity barrel vaults are applicable in meeting halls, sports stadiums, and passenger terminals. They are also implemented to cover the roof of the gathering place for many people. In the mentioned applications, in case of progressive failure in the critical members of the structure, the occurrence of great human and financial losses will be inevitable. Therefore, in this study, the critical members of the double-layer tensegrity barrel vaults are detected using finite element modeling in Abaqus software.

In progressive collapse, first, one or more members of the structure fail due to factors such as poor material, weak joints, or abnormal loads such as impact or explosion. After the initial failure, due to the redistribution of forces and its dynamic effects, some other members of the structure may fail and eventually, the structure will fail completely. Since the tensegrity structures are designed with different modules and shapes, after the initial failure occurs, generally, two possibilities exist. First, the initial failure leads to the failure of the overall structure. Second, the initial failure can be limited to the same initial failure. In other words, other members of the structure provide stability of the structure after the redistribution of forces. The type of member in which the initial failure occurred can affect the propagation of the failure in the structure. Some members can aggravate the problem due to factors such as the location and properties of the applied materials and sections. In this study, the members of the structure in which the initial failure leads to more failure in the structure and creates a more critical state for the stability of the structure are called "critical members". In the present study, a double-layer tensegrity barrel vault consisting of square modules is designed. Progressive collapse is investigated in the designed structure. The goal is to find members of the structure in which more members will fail after the initial failure and the stability of the structure will become more critical. Finally, after performing non-linear dynamic analysis, the results are presented and the critical members of the structure are introduced.

2. Finite Element Modeling

Formain software [21] is used to create the barrel vault geometry. This software is used professionally to create various geometric shapes in space structures. After defining barrel vault geometry, the output files of the Formain software are imported into Abaqus software [22].

2.1 Members modeling in Abaqus

The members of tensegrity structures are modeled as compression and tensile members. The truss element in Abaqus software is used to model each of these members.

2.2 Modeling the behavior of materials

Separate stress-strain curves according to Figures (1) and (2) are used for tensile and compression members. Tensile members have no stiffness in compressive stress. The curve of tensile members includes linear and non-linear regions. For compression members, the slenderness ratio of 100 is used. In compression members, an initial imperfection of (0.001L) is considered, where L is the length of the member. In these members, initially in a separate file, the material curve is obtained according to Figure (2) and then it is used in the models of the present study. Therefore, the behavior of compression members which also includes linear and non-linear parts. Since the analyses are non-linear and dynamic, the Rayleigh coefficient method is used to consider damping.

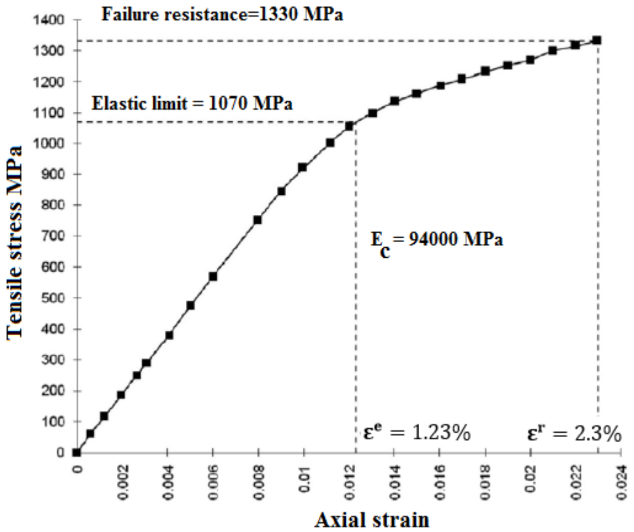

Fig. 1: The strain–stress curve of the tensile members (Shekastehband et al. [7]).

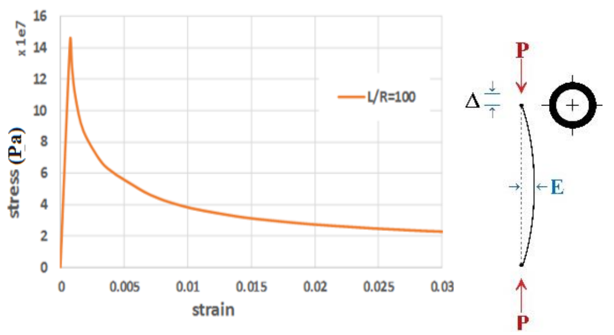

Fig. 2: The axial strain-axial stress curve of the compression members with a slenderness ratio of 100.

2.3 Modeling of member loss

In each non-linear dynamic analysis, one member is removed from the structure. Model Change settings are used in Abaqus software to delete a member. Each member is deleted within 0.0001S, where S is in seconds.

2.4 Damping in the structure

For non-linear dynamic analysis, it is necessary to enter the damping characteristics of structural materials. Therefore, before the non-linear dynamic alternative path analysis, a separate analysis is performed to determine the damping characteristics of the structure. In this analysis, each of the pre-stressing, loading, and unloading steps are applied in separate steps. Finally, a frequency analysis is performed and the damping characteristics of the structure are obtained using the frequencies of the structure.

In previous studies, the frequency of the structure in the first and fifth modes has been used to calculate the Rayleigh coefficients. The damping coefficients of truss structures are about 1 to 2.5% [23]. In dynamic analysis, Rayleigh coefficients and the time required to remove a member are obtained based on Equations (1), (2), and (3), respectively [24].

$$\alpha = \frac{2\omega_1\omega_5(0.15\omega_5-0.25\omega_1)}{\omega_5^2-\omega_1^2} \tag{1}$$

$$\beta = \frac{2(0.25\omega_5^2-0.15\omega_1^2)}{\omega_5^2-\omega_1^2} \tag{2}$$

$$\Delta T = \frac{1}{20}T_{co} \quad , T_{co} = \frac{2\pi}{\omega_\infty} \quad , \quad \omega_\infty = 4\omega_0 \tag{3}$$

Where ω_1 and ω_5 are the angular frequencies related to the first and fifth modes of vibration and ω_0 is the angular frequency related to the first mode of natural vibration of the structure.

2.5 Dynamic non-linear alternative path method

In the alternative path method, the initial failure of the structure is allowed. However, the alternative path of load transfer is provided to prevent its propagation and collapse of the structure. In this method, instead of applying any abnormal load to the structure the member is removed from the structure and it is checked whether the damaged structure can maintain its stability or not. In this study, the non-linear behavior of materials and the dynamic effects are used in alternative path analysis, therefore the structure behaves more realistically.

2.6 Nonlinear dynamic alternative path analysis steps

Before starting the steps of nonlinear dynamic alternative path analysis, the structural design steps are completed. In the first step, pre-stressing is applied to create stability in the structure. After pre-stressing, the loading of the structure is done. In the next step, the member is removed dynamically and the behavior of the structure in a dynamic step is examined for 5 seconds. This process determines whether the structure can maintain its stability after the removal of the member or suffers from total instability.

2.7 Failure mechanisms in nonlinear dynamic alternative path analysis

Two failure mechanisms are proposed in the nonlinear dynamic analysis of tensegrity structures [7]. Figure (3) shows the first type of failure mechanism. In this graph, first, the structure experiences a dynamic snap through and by reaching a new equilibrium state, it settles in its new equilibrium under the influence of damping by reducing the oscillation amplitude (partial progressive collapse). The second type of failure mechanism of tensegrity structures is shown in Figure (4). In this mechanism, the displacement of structure increases at the beginning of the graph and over time, the structure collapses. Thus, during the first type of failure mechanism, the structure remains in its new equilibrium by experiencing the initial instability, however in the second type of tensegrity structure's failure mechanism, the instability of the structure leads to the collapse of the structure (full progressive collapse).

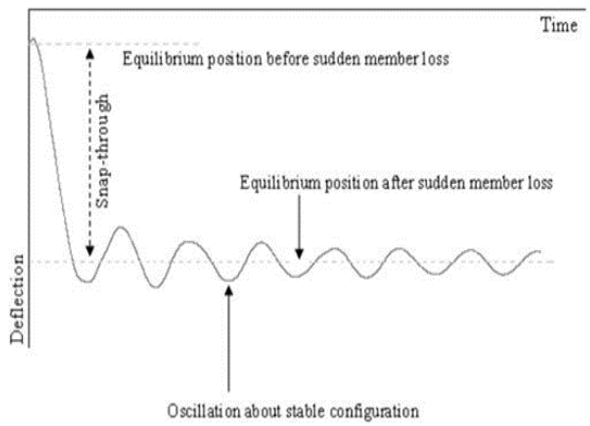

Fig. 3: Schematic representation of partial progressive collapse [7].

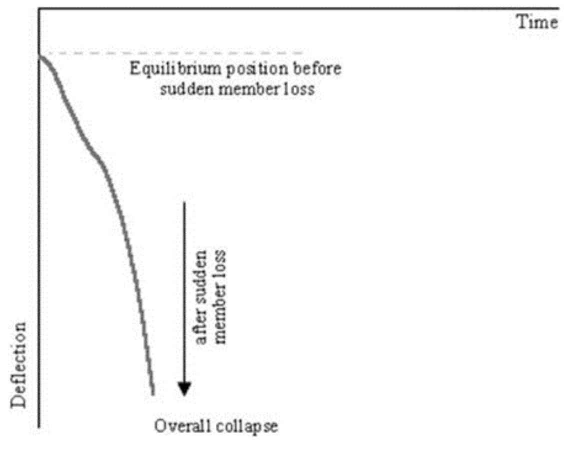

Fig. 4: Schematic representation of full progressive collapse [7].

2.8 Finite element modeling verification

The verification model is based on numerical work performed by Shekastehband et al. [7]. In their work, the sensitivity analysis of tensegrity structures to removing members has been done. To ensure the accuracy of the performed analysis, the different stages of the analysis are compared. The verification model is a double-layer tensegrity grid consisting of 36 square modules which are connected by node to node according to Figure (5). The length and height of the mentioned tensegrity grid are 9m and 1.15m, respectively. Compression and tensile members in the upper, lower, and middle layers are named S, U, L, and B, respectively. In Figures (6) and (7), the comparison between material behavior of compression members and axial stress of the members after pre-stressing of the developed numerical modeling in Abaqus software and numerical modeling results by Shekastehband et al. [7] are shown. In another step of verification, nonlinear dynamic analyses were performed by removing some members and time-displacement curves were obtained and these curves were compared with the results of Shekastehband et al. [7] in Figures (8) and (9). Figure (8) indicates that removing the L1-M8 member of the structure has led to the total collapse of the structure. Therefore, it is according to the second type of failure mechanism. Figure (9) shows that the removal of the L3-M8 member did not lead to instability in the structure and the amplitude of oscillation of the structure gradually decreased due to damping. As shown in Figures (6-9), the results obtained from FE modeling in Abaqus software have good agreement with the numerical results of Shekastehband et al. [7].

3. Studied Tensegrity Systems

The flowchart of steps taken into account this paper to identify critical members in a tensegrity barrel vault is shown in Figure (10).

3.1 Constituent module

The geometry of the tensegrity barrel vault studied in this paper is shown in Figure (11). This structure consists of square modules. The square modules are connected by node-to-node connections. The dimensions of the modules are 1.5×1.12×1.12 m. In these modules, there are compression members with lengths of 1.77 and 1.79 m and tensile members with lengths of 1.12, 0.824, and 1.37 m.

3.2 Dimensions of barrel vaults

According to Figure (11), the studied barrel vault consists of 11 modules along the barrel vault span and 14 modules in the longitudinal direction. The length of the barrel vault is 15.68m. The span is 12 m and the height to span ratio is 0.1.

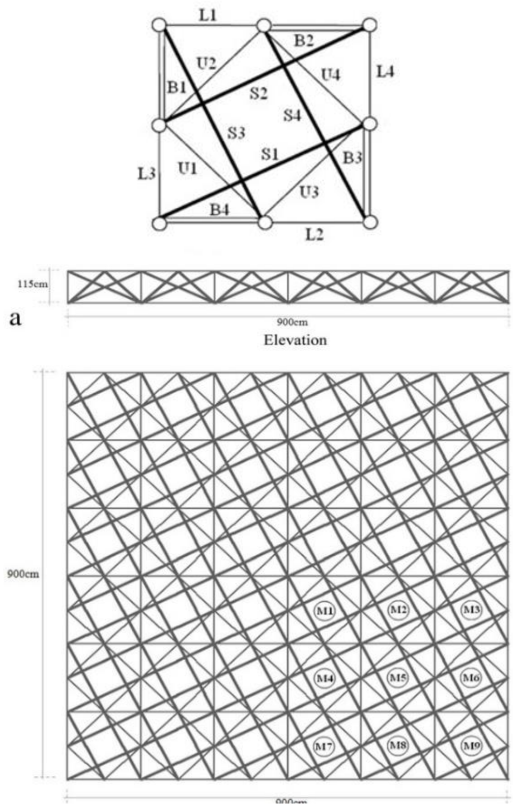

Fig. 5: Two-layer tensegrity grid studied by Shekasteband et al. [7].

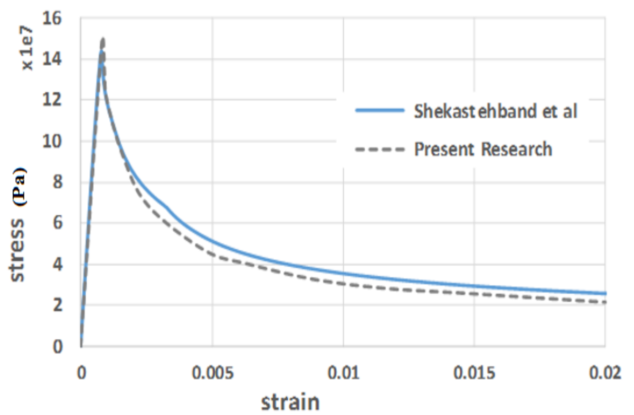

Fig. 6: Comparison of the behavior of compression members obtained from Abaqus software with the results of Shekastehband et al. [7].

3.3 Material specifications

For tensile members, cable sections are used based on the material specifications obtained in the experimental research of Shekastehband et al. [7] (Figure (1)). Tubular sections (hollow circles) are used for compression members. In compression members, a slenderness ratio of 100 and an initial imperfection are considered in the middle of their length. Therefore, the graph in Figure (2) is used for the specifications of materials of compression members. Both geometric and material nonlinearities are considered in this study. In Abaqus software, the BEEM element is used for modeling the compression (with a modulus of elasticity of 2E11 and the Poisson's ratio of 0.3) and tensile (with a modulus of elasticity of 9.8E10 and the Poisson's ratio of 0.3) members.

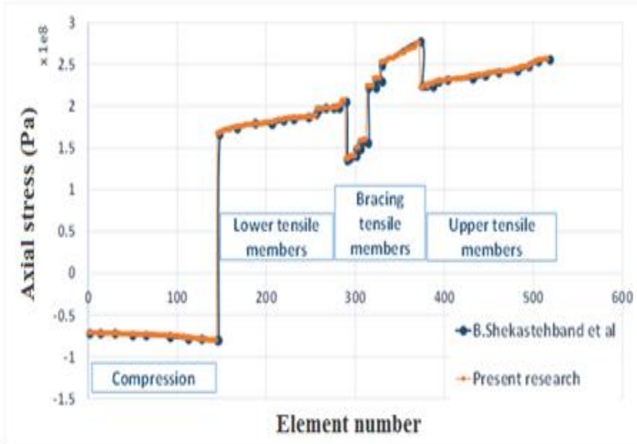

Fig. 7: Comparison of the axial stress of the elements after pre-stressing obtained from Abaqus software with the results of Shekastehband et al. [7].

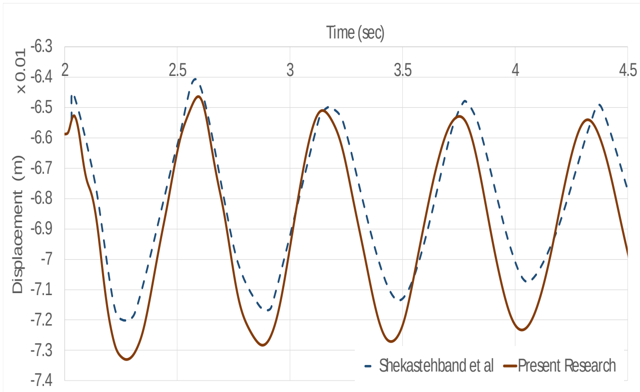

Fig. 8: Comparison of the time-displacement curve of the structure corresponding to dynamic removal of L1-M8 member obtained from Abaqus software with the results of Shekastehband et al. [7].

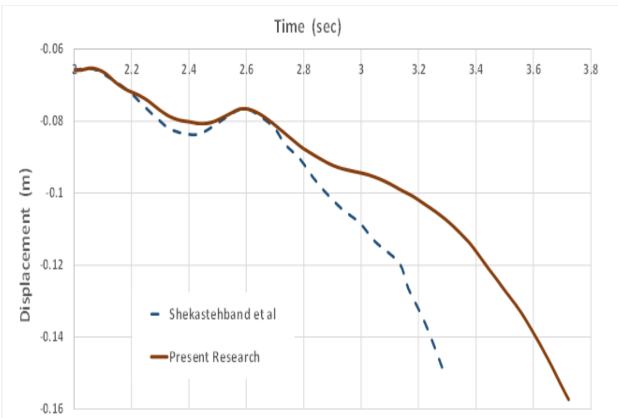

Fig. 9: Comparison of the time-displacement curve of the structure corresponding to dynamic removal of L3-M8 member obtained from Abaqus software with the results of Shekastehband et al. [7].

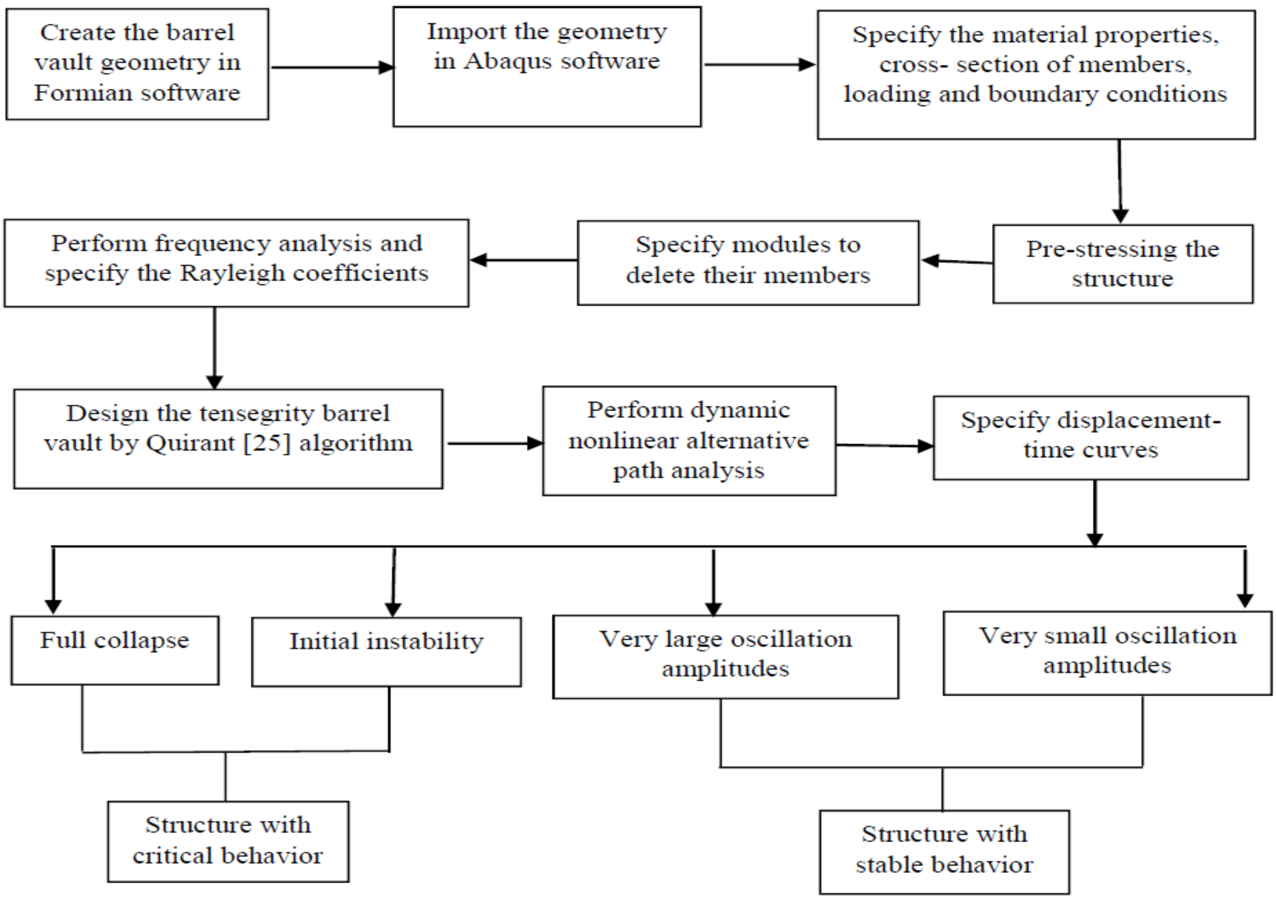

Fig. 10. The flowchart of steps taken in this paper to identify critical members in a tensegrity barrel vault.

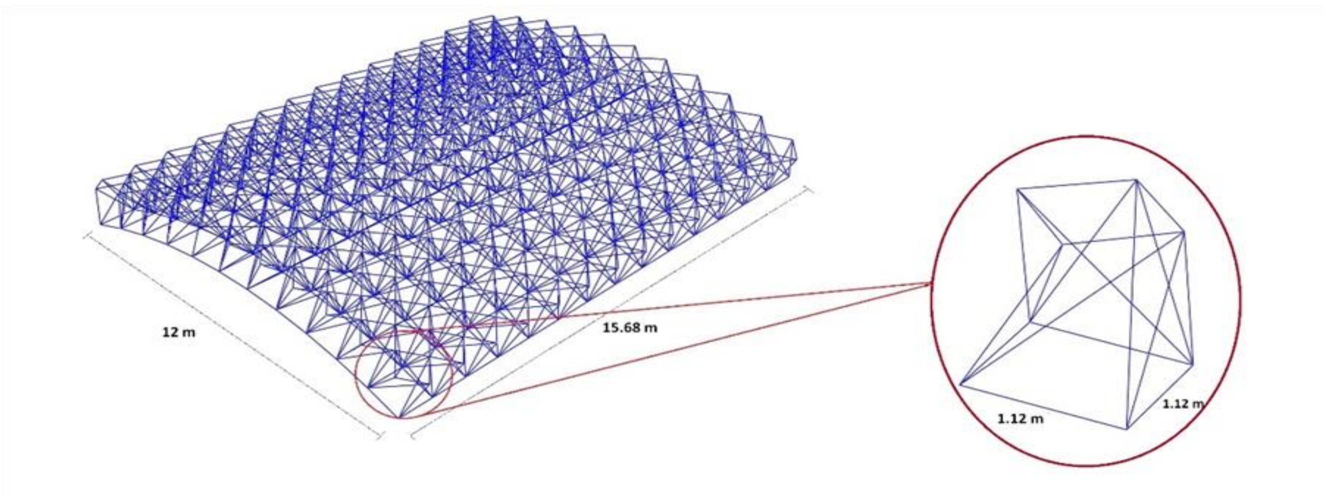

Fig. 11: The configuration of the studied barrel vault and its constituent square module.

3.4 Structural design

To design the tensegrity barrel vault structure, the algorithm proposed by Quirant [25] is used. Accordingly, two load combinations are presented. In the first load combination (G + Q + S), Q, G, and S represent the snow load, dead load, and the load due to the pre-stressing of the structure, respectively. In the first load combination, the maximum deformation of the structure should not exceed 1/200 of the span. Moreover, under the second load combination (1.35G + 1.5Q + 1.2S), the overall stability of the structure is maintained and does not suffer partial or total collapse. In the studied tensegrity barrel vault, the tensile members have a cross-sectional area of 7.15 cm^2 and an external radius of 1.64 cm .Whereas, compression members have an area of 7 cm^2 and internal and external radius of 2.28 and 2.72 cm, respectively.

3.5 Loading of structure

Structural loading includes dead and snow loads. According to Figure (12), the load is applied to all nodes of the upper layer of the structure (There are 333 nodes in the top layer of the barrel vault). The value of dead and snow loads are 300 and 1050 N/m^2, respectively. Due to performing the dynamic analysis, the dead and snow loads on each node are entered as a mass. Assuming a gravitational acceleration of 9.806 m/s^2, the dead and snow loads applied on each node are 17.3451 and 61.2182 kg, respectively.

3.6 Support conditions

The boundary nodes in the lower layer of the barrel vault in its longitudinal direction are the structural supports (Figure 13).

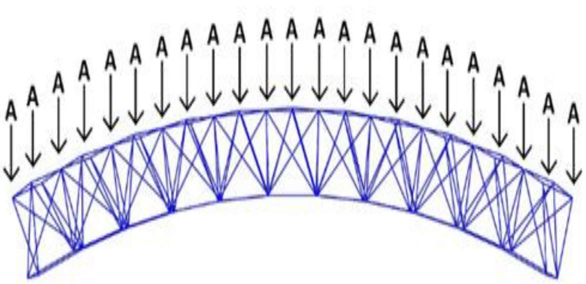

Fig. 12: The distribution of dead load in the studied tensegrity barrel vault

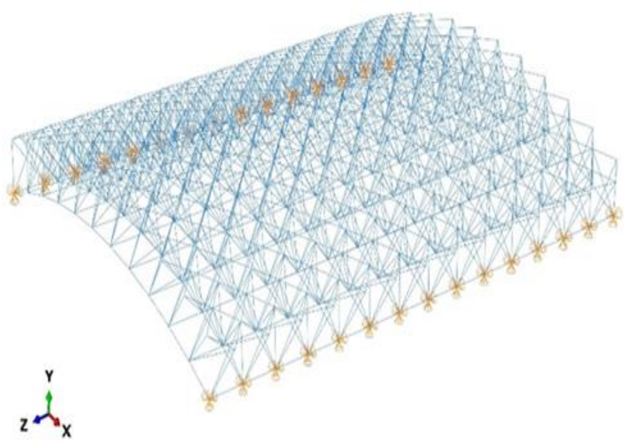

Fig. 13: Support conditions in the studied tensegrity barrel vault

3.7 Pre-stressing method

Tensegrity structures cannot maintain their stability before pre-stressing. Therefore, initial stress is applied to the cable members of the tensegrity structure. The method presented by Quirant [25] is used to determine the amount of initial stress. Accordingly, the maximum pre-stressing of the structure should be in a way that the average total stress of the compression members by the application of initial stress is a maximum of 50% of the buckling limit of the compression members of the structure. Pre-stressing is performed using the settings of the PREDIFINED FIELD MANAGER section located in Abacus software.

Figure (14) shows the axial stress of different members of the barrel vault after pre-stressing.

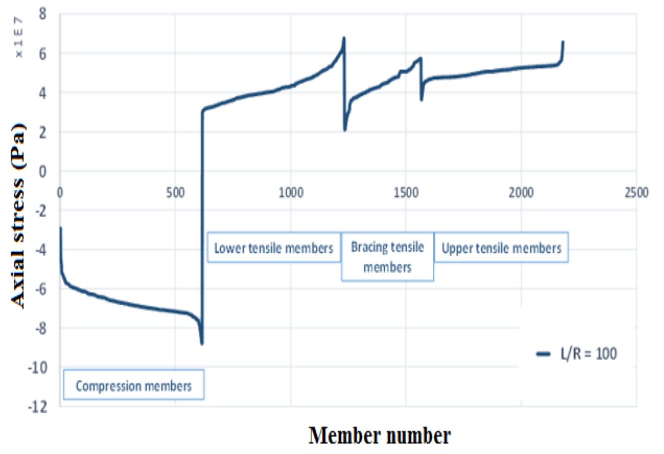

Fig. 14: Axial stress of different structural members

3.8 Position of selected modules to delete members

Due to the geometric symmetry of the studied structure, a certain number of structural members are used to perform the intended analysis. Therefore, six modules along the span and seven modules along the length of the barrel vault are selected. The location of the selected modules is shown in Figure (15). Moreover, the numbering of the selected modules and the naming of the module members are according to Figures (16) and (17), respectively.

3.9 Loading level

In this study, the structure is loaded under the combined load combination (G + Q + S). This load combination is already introduced in section (3.4).

3.10 Number of analyses

In each dynamic analysis, only one member of the structure is eliminated. Therefore, according to Table 1, 594 nonlinear dynamic alternative path analyses are performed for 594 members studied in this study.

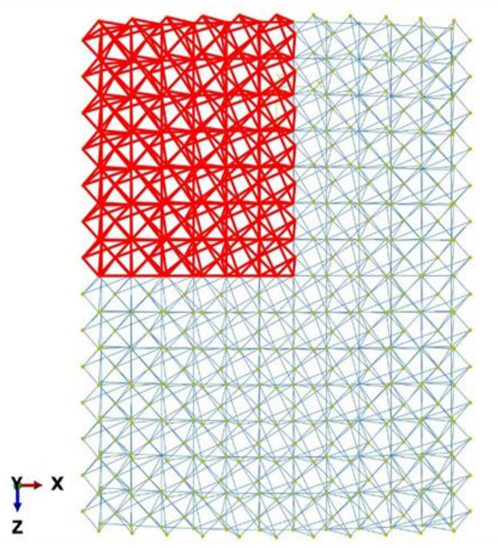

Fig. 15: Position of the modules selected to delete members

M1	M2	M3	M4	M5	M6
M7	M8	M9	M10	M11	M12
M13	M14	M15	M16	M17	M18
M19	M20	M21	M22	M23	M24
M25	M26	M27	M28	M29	M30
M31	M32	M33	M34	M35	M36
M37	M38	M39	M40	M41	M42

Fig. 16: Numbering of selected modules

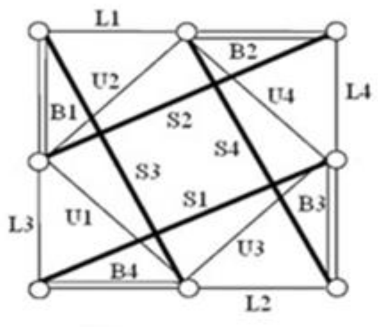

Fig. 17: Naming of the module members

Table 1: Number of analyzes in each type of barrel vault member

S	U	B	L	SUM
168	168	168	90	594

3.11 Target point

According to previous studies [7], the central node in the upper layer of the barrel vault is used as the target point to investigate the behavior of the structure.

3.12 Remove a member of barrel-vault

According to previous studies [7], the rate of accident and the initial failure of the member is up to the maximum level of 0.1T, in which T is the natural time period of the structure with the removed member. Based on the work of Habibi and Ghandi [17], the above duration in the present analysis is considered 0.0001 seconds. To apply the deletion settings, in a separate step as DYNAMIC IMPLICIT, the MODEL CHANGE settings are used, and the deletion is performed.

4. Numerical results

By performing the analysis, three cases may take place for the structure. In the first case, removing the member does not lead to local or total instability, and the structure maintains its stable state. In the second case, as shown in Figure (3), the structure experiences local instability after the removal of the member; however, it regains its steady state. In the third case, according to Figure (4), the removal of the member causes the structure to go from steady state to total instability, and the structure collapses. In the first and second cases, in addition to the removed member, other members may lose their strength; however, the alternative path is formed by other members of the structure, and the structure regains its stability. In the third case, the initial failure starts from one member and leads to the failure of several other members and eventually, the collapse of the structure. Based on the analysis results, in this study, the first and second cases are observed. However, the third case is not observed. The results of the analysis are given in Table 2. For the convenience of viewing the results, the abbreviation S (Stable) (to express the first state of structural behavior after the removal of a member) and I.U (Initial unstable) (to express the second state of structural behavior after the removal of a member) are used. In some analyses, the beginning and the end of the removed member are located between the two supports. Therefore, the removal of this member will not have effect on the failure of other members and the stability of the structure. The symbol N.E (NO EFFECT) is used for this type of analysis.

Table 2 shows that:

- In most cases of removal members, the stability of structures is maintained, and in some cases, initial instability has occurred. In none of the cases, total instability occurr.
- In most cases, in each of the longitudinal and transverse directions of the tensegrity barrel vault, a greater number of

initial instability behaviors are observed by moving toward the middle modules.

- The steady state prevails in the analysis related to Modules 23 and earlier, and the initial instability behavior is observed in Modules 24 and later.
- During the removal of various members of modules 41 and 42, the structure has more critical behavior than other modules, and more initial instability is observed than other modules.
- In Table 2, the members of the structure that have the maximum stress under static loading are marked with an orange background color. According to the obtained results, removing members in none of the above cases will lead to initial or total instability.
- Removing member B1 only shows instability in module 42. Also, in the case of L3 removal, instability is observed only in modules 41 and 42.
- In each U2 and U4 removal modes, instability is observed in the eight analyses, which is the highest instability among the module members.
- By removing the upper layer tensile members (U), instability is observed in 25 analyzes, and by removing the lower layer (L) tensile members, instability is observed in 9cases. As a result, removing members U and L creates the maximum and the minimum number of initial instabilities, respectively.
- Module 42, with 14 instability modes, has the highest number of instability modes among the selected modules.

In Figure (18), the members whose removal has led to the initial instability in the structure (in red color) are seen among all the members selected for removal. In Figure (19), all the members marked in red in Figure (18) are observed among all the members of the structure. According to Figures (18) and (19), it can be said that as we approach the middle of the cask, the number of members whose removal leads to the initial instability of the structure increases.

Figure (20) shows the displacement -time curves (obtained from nonlinear dynamic analysis) of barrel-vault due to the loss of some members of the M3 module. In the above curves, the structure suffers from initial, local, or total instability in none of the analyses. In most of the obtained curves in all the analyzed modules, the important event occurs in the range of 2 to 3 seconds. Therefore, it is avoided to present the curve in the range of 4 to 5 seconds, and only the range of 2 to 4 seconds is provided.

Figure (21) shows the displacement-time curves for the removal of some members of the M7 module. These curves do not show total and initial instability. In the curves related to the removal of S2 and U2 members, after the removal of the member, the structural analysis was stopped by creating local instability in the position of the removed member. To solve this problem, the load related to the node connected to the deleted member is removed, and the curve is obtained in the mentioned members. Therefore, nonlinear dynamic analysis of members S2 and U2 have local instability.

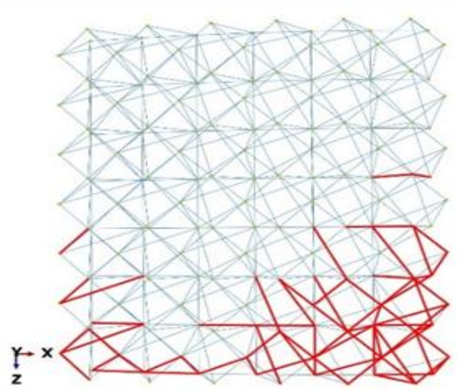

Fig. 18: The members whose removal has led to the initial instability among all the members selected for removal.

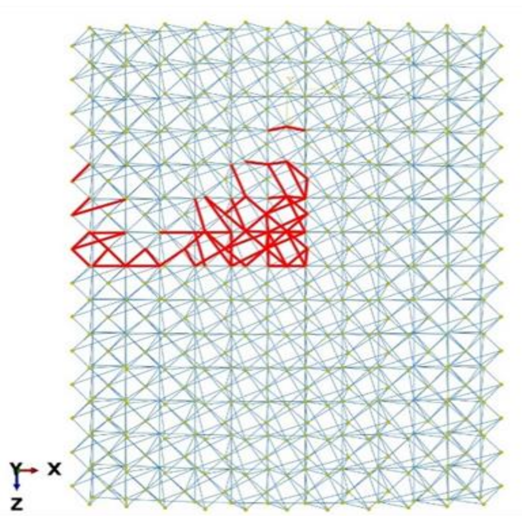

Fig. 19: Members whose removal has led to initial instability among all the members of the structure.

Figures (22) and (23) show the displacement-time curves of barrel-vault due to the loss of some members of the M18 and M20 modules, respectively. In these Figures, the steady state is maintained in all the curves, and no significant oscillation is observed.

Figure (24) shows the displacement-time curves for removing some members of the M30 module. Module M42 is the middle module of the barrel vault along the longitudinal and span directions, and module M30 is adjacent to module M42. According to Figure (24), the curves corresponding to U4, S4 ,and B3 members are associated with initial instability afterward reach their steady state with the effect of damping and reduction of the oscillation amplitude. Figure (25) shows the displacement-time curves for the removal of some members of the M36 module. As shown in this figure, the curve corresponding to removing the B2 member has no instability. However, the corresponding curves related to removing L3, U4, and S2 are associated with initial instability. In the curve corresponding to U4, the displacement of the structure at the target point decreases after the removal of the member and subsequent initial instability. However, in the curves corresponding to L1 and S4, the structural displacement increases at the target point after the initial instability in the barrel vault. Therefore, in Figure (25), despite the initial instability, the stability of the structure is maintained under the effect of structural damping.

Table 2: The stability status of each of the analyses performed in the present study.

	U4	U3	U2	U1	L3	L2	L1	S4	S3	S2	S1	B4	B3	B2	B1
M1	S	S	S	S	N.E	-	S	S	S	S	S	S	S	S	S
M2	S	S	S	S	S	-	S	S	S	S	S	S	S	S	S
M3	S	S	S	S	S	-	S	S	S	S	S	S	S	S	S
M4	S	S	S	S	S	-	S	S	S	S	S	S	S	S	S
M5	S	S	S	S	S	-	S	S	S	S	S	S	S	S	S
M6	S	S	S	S	S	-	S	S	S	S	S	S	S	S	S
M7	S	S	S	S	N.E	-	S	S	S	S	S	S	S	S	S
M8	S	S	S	S	S	-	S	S	S	S	S	S	S	S	S
M9	S	S	S	S	S	-	S	S	S	S	S	S	S	S	S
M10	S	S	S	S	S	-	S	S	S	S	S	S	S	S	S
M11	S	S	S	S	S	-	S	S	S	S	S	S	S	S	S
M12	S	S	S	S	S	-	S	S	S	S	S	S	S	S	S
M13	S	S	S	S	N.E	-	S	S	S	S	S	S	S	S	S
M14	S	S	S	S	S	-	S	S	S	S	S	S	S	S	S
M15	S	S	S	S	S	-	S	S	S	S	S	S	S	S	S
M16	S	S	S	S	S	-	S	S	S	S	S	S	S	S	S
M17	S	S	S	S	S	-	S	S	S	S	S	S	S	S	S
M18	S	S	S	S	S	-	S	S	S	S	S	I.U	S	S	S
M19	S	S	S	S	N.E	-	S	S	S	S	S	S	S	S	S
M20	S	S	S	S	S	-	S	S	S	S	S	S	S	S	S
M21	S	S	S	S	S	-	S	S	S	S	S	S	S	S	S
M22	S	S	S	S	S	-	S	S	S	S	S	S	S	S	S
M23	S	S	S	S	S	-	S	S	S	S	S	S	S	S	S
M24	S	S	S	S	S	-	S	S	S	S	S	I.U	S	I.U	S
M25	S	S	I.U	S	N.E	-	S	S	S	S	S	S	S	S	S
M26	S	S	S	S	S	-	S	S	S	S	S	S	S	S	S
M27	S	S	S	S	S	-	S	S	S	S	S	S	S	S	S
M28	S	S	S	S	S	-	S	S	S	S	S	S	S	S	S
M29	S	S	S	S	S	-	S	S	I.U	S	S	S	S	I.U	S
M30	I.U	S	S	S	S	-	S	I.U	I.U	S	S	I.U	I.U	S	S
M31	S	S	I.U	S	N.E	-	S	S	S	I.U	S	S	S	S	S
M32	S	S	S	S	S	-	S	S	S	S	S	S	S	S	S
M33	S	S	S	S	S	-	S	S	S	S	S	S	S	S	S
M34	I.U	S	S	S	S	-	S	I.U	I.U	S	S	S	S	S	S
M35	I.U	I.U	I.U	I.U	S	-	S	S	I.U	S	S	S	I.U	S	S
M36	I.U	I.U	I.U	I.U	S	-	S	I.U	S	I.U	I.U	S	S	I.U	S

M37	I.U	S	I.U	I.U	S	I.U	I.U	S	S	I.U	I.U	S	I.U	S	S
M38	S	S	S	S	S	I.U	S	S	S	S	I.U	S	I.U	S	S
M39	S	S	S	S	S	S	S	S	S	S	I.U	S	I.U	S	S
M40	I.U	S	I.U	S	S	S	I.U	I.U	I.U	S	I.U	S	S	S	S
M41	I.U	I.U	I.U	I.U	I.U	S	S	S	S	I.U	S	S	S	I.U	S
M42	I.U	I.U	I.U	I.U	I.U	I.U	I.U	I.U	I.U	I.U	S	I.U	I.U	I.U	I.U

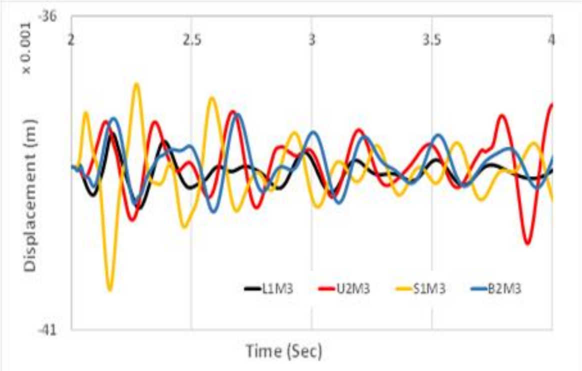

Fig. 20: Displacement -time response of barrel-vault due to the loss of some members of the M3 module.

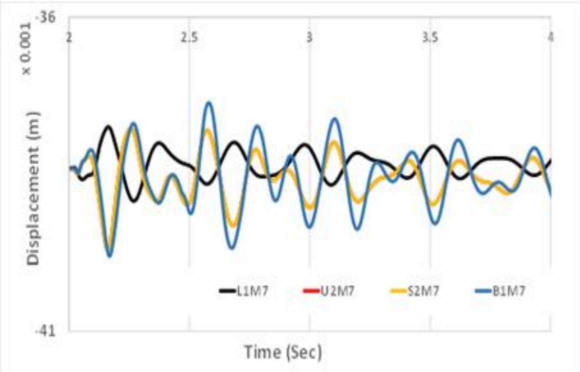

Fig. 21: Displacement -time response of barrel-vault due to loss of some members of the M7 module.

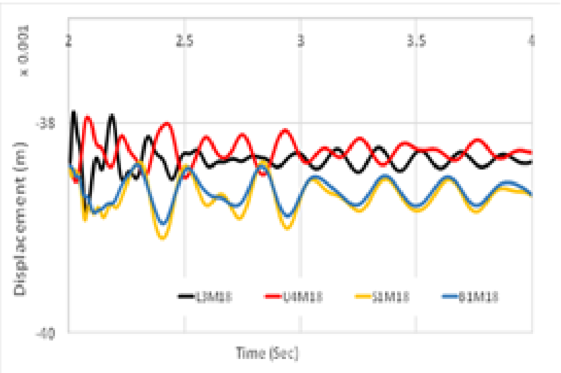

Fig. 22: Displacement -time response of barrel-vault due to the loss of some members of the M18 module.

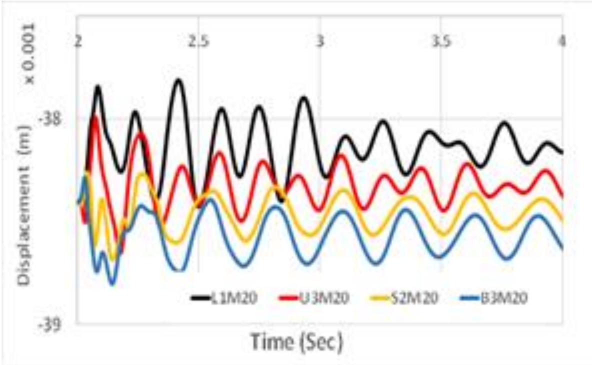

Fig. 23: Displacement -time response of barrel-vault due to the loss of some members of the M20 module.

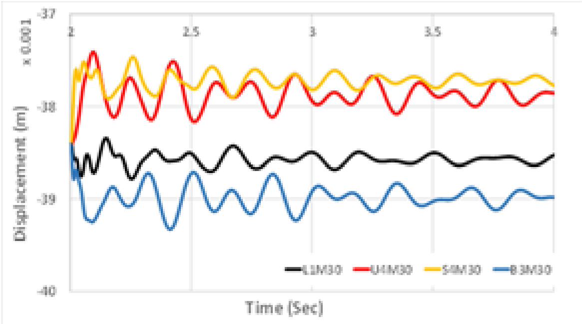

Fig. 24: Displacement -time response of barrel-vault due to the loss of some members of the M30 module.

Figure (26) shows the displacement-time curves corresponding to the removal of some members of the M37 module. According to this Figure, the curve corresponding to the removal of L2 is associated with a reduction in displacement due to the initial instability. Then, under the damping effect on the behavior of the structure, it becomes stable. In the curve corresponding to the removal of B3, the initial instability occurs first, afterward the stability of the structure is maintained by increasing the displacement of the target point. In the case of curves corresponding to the removal of S2 and U2 members, it should be noted that local instability has occurred in them. To prevent Abaqus from stopping the analysis (due to local instability), in S2 analysis, the load corresponding to the node connected to the member is removed, and in U2 analysis, the load and the members connected to the node that has become unstable by removing the member, are removed. In some members of the boundary modules, by removing the member, the remaining members cannot establish the stability of the node attached to the deleted member.

Therefore, the analysis is stopped by Abaqus. To solve this problem and the possibility of continuing the analysis process by Abaqus, considering that the removal of the desired member has caused local instability in the structure, the selected node is removed, and the analysis continues. Accordingly, in the curves corresponding to the removal of the S2 and U2 members, the initial instability is observed after the removal of the member. In Figure (26), the initial displacement of the structure in modes S2, U2, and B3 shows a slight increase, but generally, according to the definition of initial instability, it is one of the mentioned cases. The structure does not suffer from total instability in any of the curves in Figure (26). According to the curves in Figure (27), which are related to the removal of some members of the M38 module, the removal of S1 and B3 members, is associated with initial instability and afterward maintains its stability by increasing the displacement of the target point of the barrel vault. In the curve corresponding to L2, the initial instability in the structure has led to less displacement in the structure. Hence, the oscillation of the structure is controlled by damping effects, and the structure maintains its stability. The curve corresponding to the removal of the U1 member shows the lowest amplitude of oscillation among the other curves, and the structure is not affected by the removal of the U1 member.

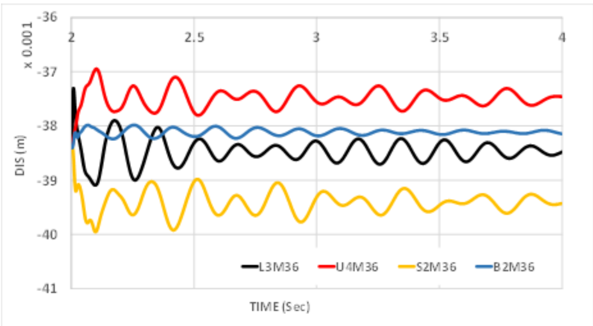

Fig. 25: Displacement -time response of barrel-vault due to the loss of some members of theM36 module.

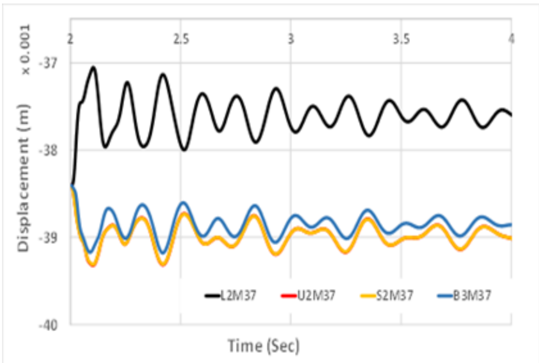

Fig. 26: Displacement -time response of barrel-vault due to the loss of some members of the M37 module.

Figure (28) shows the displacement-time curves related to the removal of some members of the M39 module. In this figure, the curves corresponding to the L1, B3, and S1 members are associated with initial instability, and the curve corresponding to the U3 member has no instability. As can be seen from Figure 29, all displacement-time diagrams related to the removal of members of the M40 module are associated with the initial instability. By the initial instability, the structure regains its stability and none of the initial instabilities leads to total collapse.

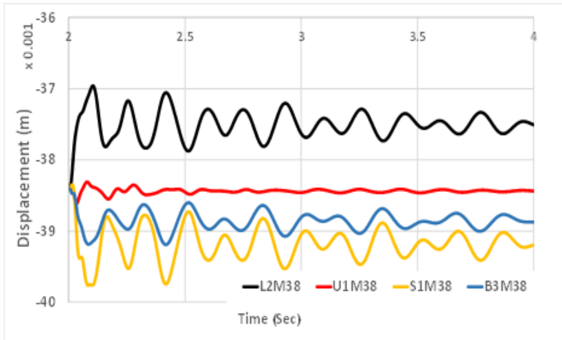

Fig. 27: Displacement -time response of barrel-vault due to loss of some members of M38 module.

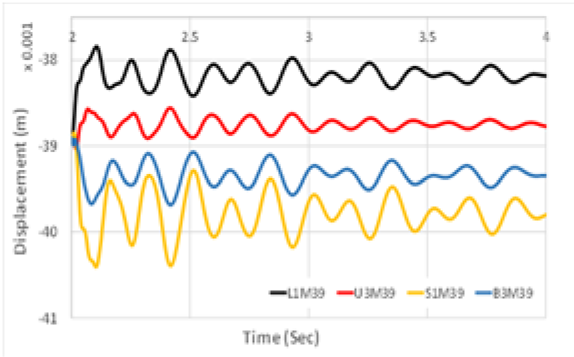

Fig. 28: Displacement -time response of barrel-vault due to loss of some members of M39 module.

As shown in Figure (30), the displacement-time curves corresponding to the removal of L3, U4 ,and S1 members of the M41 module are associated with instability ,and the curve corresponding to the removal of the B3 member is stable and, like other modules, no total collapse occurs in any case of the member removing in this module. As mentioned earlier, among the considered modules, the M42 module is the most central module. Figure (31) shows the displacement-time curves corresponding to the removal of L3, U2, S3, and B1 members of this module. As shown in the figure, all curves are associated with initial instability. However, removing none of the members leads to total collapse.

Table 3 shows the maximum oscillation amplitude for any member, in which the nonlinear alternative path analysis has been performed. Due to the large numbers and for the convenience of using the results of the above table, the numbers in Table 3 are normalized with the largest value and are presented in Table 4. In Table 3, the largest displacement is related to the removal of the S3 member in the M42 module, and its value is equal to 6.29 mm. Therefore, normalizing the numbers in the table with the mentioned number is done, and the results are presented in Table 4.

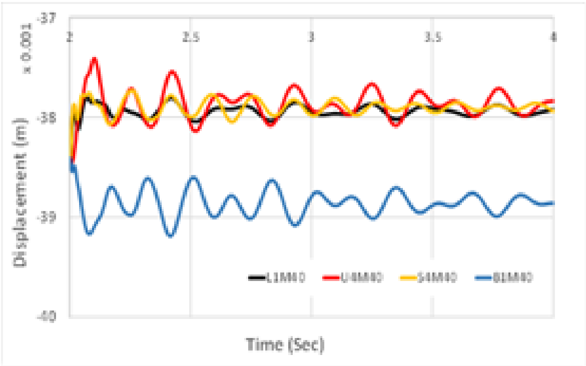

Fig. 29: Displacement -time response of barrel-vault due to loss of some members of the M40 module.

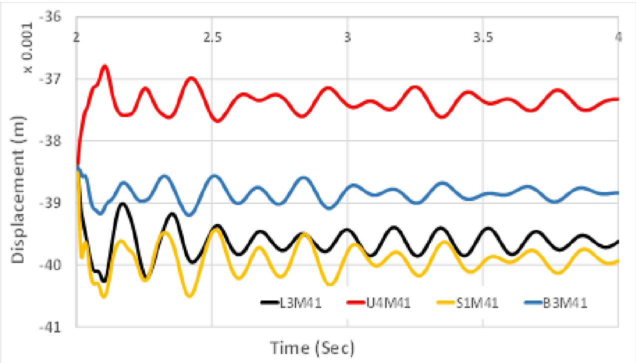

Fig. 30: Displacement -time response of barrel-vault due to loss of some members of the M41 module.

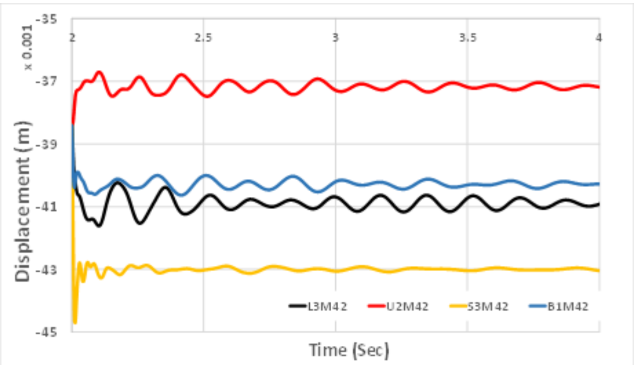

Fig. 31: Displacement -time response of barrel-vault due to loss of some members of the M42 module.

In reviewing the results of Table 4, the following results are presented:

1) In most cases, the displacement percentage is less than 10%.

2) In some cases, despite maintaining the stability of the structure (without the initial instability), the displacement has increased up to about 50%, and it is even more than cases where the initial instability happens.

3) Creating initial instability in the structure does not necessarily involve significant displacement.

4) The highest displacement is observed in the analysis resulting from the removal of members M42 and M1.

5) In module M1, although the initial instability is observed in none of the cases of removing its members, the relative displacement is higher.

6) The least displacement is related to the modules in the range of M9 to M28.

7) The least amount of displacement has occurred in the cases of removing B4 and B2 members.

8) The maximum displacement has occurred in the cases of removing L2 and S1 members.

9) Among the module layers (L, B, S, and U), the removal of S and U members has led to the most displacement in the structure; moreover, the removal of B members has led to the least displacement.

10) The color of the red box denotes the analysis in which the initial instability occurred.

11) The purple background color represents the analysis in which the initial instability in the members of the boundary modules has occurred, and to prevent halting the analysis by the software, the members of the boundary node connected to the desired member are removed. According to the table, this happened once, three times, and once in U4, U2, and B2 members, respectively.

12) The green background signifies the analysis that the displacement of the structure has decreased at its control point after the removal of the desired member. The decline may have occurred in the oscillation amplitude or during an initial instability. For example, B2M18, U2M27, and U2M28 analyses are examples of oscillation amplitude reductions, and B4M42, L1M34, and U2M30 analyses are examples of results that the structural displacement is reduced by the initial instability.

13) According to Table 4, in a number of analyses, the structure displacement after member removal was less than the same value exactly before removing the member. U1, U2, U3, U4, and L1 members had the highest displacement reductions, and B1, B3, S1, S2, S3, and L3 members were less influenced. This case is unexpected and confirms the conclusion obtained by Habibi and Ghandi [17] that in nonlinear static analysis of some cases, in fixed displacement, the bearing capacity of the structure with the removed member is more than the structure without removing the members. It seems that the result is related to the problem of structural optimization. Therefore, it is necessary to perform comprehensive research on this issue.

Table 3: Maximum oscillation amplitude for the responses corresponding to the deleted members in nonlinear dynamic analysis.

U4	U3	U2	U1	L3	L2	L1	S4	S3	S2	S1	B4	B3	B2	B1	
1.36E-03	2.71E-03	1.35E-03	1.89E-03	0.00E+00	-	9.73E-04	1.32E-03	1.98E-03	1.44E-03	3.57E-03	7.02E-04	8.05E-04	1.31E-03	1.45E-03	M1
9.86E-04	1.54E-03	9.91E-04	1.26E-03	1.07E-03	-	7.99E-04	5.89E-04	7.66E-04	7.52E-04	3.08E-03	3.71E-04	8.07E-04	7.85E-04	2.03E-03	M2
9.87E-04	7.69E-04	1.22E-03	8.33E-04	4.64E-04	-	6.56E-04	5.22E-04	6.23E-04	7.44E-04	1.96E-03	8.71E-05	5.60E-04	8.40E-04	5.35E-04	M3
9.87E-04	6.57E-04	3.64E-04	5.27E-04	5.92E-04	-	5.80E-04	3.64E-04	3.33E-04	5.65E-04	1.40E-03	1.11E-04	4.08E-04	8.40E-04	3.18E-04	M4
1.09E-03	5.89E-04	1.04E-03	4.70E-04	6.67E-04	-	6.48E-04	3.03E-04	2.17E-04	5.11E-04	9.05E-04	1.63E-04	3.24E-04	8.40E-04	4.09E-04	M5
9.46E-04	4.21E-04	8.14E-04	4.44E-04	7.31E-04	-	5.16E-04	2.38E-04	2.09E-04	7.22E-04	7.66E-04	2.60E-04	3.65E-04	6.48E-04	3.42E-04	M6
1.02E-03	1.05E-03	1.28E-03	1.20E-03	0.00E+00	-	6.57E-04	4.18E-04	9.29E-04	1.28E-03	5.12E-04	2.60E-04	1.91E-04	8.40E-04	1.40E-03	M7
6.16E-04	5.80E-04	1.46E-03	8.96E-04	5.07E-04	-	3.44E-04	6.15E-04	6.07E-04	1.08E-03	7.79E-04	2.38E-04	5.63E-04	2.33E-04	5.38E-04	M8
5.53E-04	4.76E-04	6.46E-04	6.29E-04	4.08E-04	-	2.67E-04	3.64E-04	4.27E-04	7.29E-04	6.15E-04	2.13E-04	4.40E-04	2.04E-04	6.21E-04	M9
3.68E-04	5.08E-04	6.55E-04	5.61E-04	4.72E-04	-	1.76E-04	3.69E-04	4.79E-04	5.76E-04	5.50E-04	1.39E-04	3.32E-04	2.04E-04	4.65E-04	M10
2.72E-04	5.01E-04	6.20E-04	3.74E-04	4.48E-04	-	1.49E-04	3.80E-04	4.63E-04	4.22E-04	4.89E-04	1.57E-04	3.90E-04	1.28E-04	3.69E-04	M11
3.21E-04	4.22E-04	5.22E-04	2.49E-04	3.84E-04	-	2.23E-04	5.50E-04	3.78E-04	6.19E-04	5.62E-04	2.24E-04	5.13E-04	1.50E-04	4.40E-04	M12
5.48E-04	6.02E-04	6.86E-04	6.38E-04	0.00E+00	-	4.42E-04	2.52E-04	6.38E-04	5.89E-04	7.95E-04	1.74E-04	3.71E-04	1.14E-04	7.24E-04	M13
5.27E-04	4.81E-04	8.06E-04	4.16E-04	3.16E-04	-	4.20E-04	3.24E-04	2.52E-04	5.16E-04	5.84E-04	1.32E-04	5.23E-04	2.43E-04	2.32E-04	M14
5.11E-04	5.19E-04	6.38E-04	5.50E-04	4.68E-04	-	3.77E-04	1.79E-04	3.99E-04	5.28E-04	4.29E-04	8.97E-05	4.15E-04	1.85E-04	4.27E-04	M15
4.51E-04	5.55E-04	6.55E-04	5.06E-04	6.13E-04	-	2.74E-04	3.24E-04	4.65E-04	5.14E-04	4.46E-04	1.19E-04	4.00E-04	1.68E-04	3.88E-04	M16
3.63E-04	5.58E-04	6.09E-04	4.40E-04	5.80E-04	-	1.98E-04	4.07E-04	3.79E-04	7.82E-04	5.45E-04	2.23E-04	5.07E-04	1.92E-04	3.68E-04	M17
4.63E-04	4.44E-04	5.40E-04	3.40E-04	5.09E-04	-	1.82E-04	4.94E-04	2.60E-04	4.94E-04	6.90E-04	2.40E-04	5.68E-04	2.02E-04	5.52E-04	M18
4.64E-04	4.20E-04	4.93E-04	4.89E-04	0.00E+00	-	4.58E-04	3.09E-04	4.63E-04	2.80E-04	9.07E-04	1.34E-04	5.02E-04	9.80E-05	5.73E-04	M19
3.19E-04	4.11E-04	5.71E-04	3.36E-04	3.01E-04	-	5.93E-04	1.06E-04	2.45E-04	1.28E-03	6.89E-04	1.20E-04	3.99E-04	8.04E-05	3.78E-04	M20
4.47E-04	5.00E-04	6.26E-04	3.40E-04	5.76E-04	-	5.10E-04	2.15E-04	3.11E-04	3.15E-04	7.17E-04	7.56E-05	4.27E-04	7.18E-05	3.42E-04	M21
4.94E-04	5.70E-04	6.75E-04	4.60E-04	7.66E-04	-	3.50E-04	2.74E-04	4.48E-04	3.98E-04	6.27E-04	7.98E-05	5.01E-04	1.88E-04	3.54E-04	M22
5.38E-04	6.29E-04	6.31E-04	5.30E-04	7.62E-04	-	2.34E-04	5.23E-04	4.09E-04	5.75E-04	6.79E-04	2.88E-04	5.85E-04	2.69E-04	4.30E-04	M23
6.82E-04	5.38E-04	5.54E-04	4.98E-04	6.71E-04	-	6.97E-04	5.99E-04	2.65E-04	9.75E-04	7.63E-04	3.19E-04	7.18E-04	2.26E-04	6.64E-04	M24
3.83E-04	3.80E-04	4.94E-04	4.93E-04	0.00E+00	-	8.03E-04	2.40E-04	3.35E-04	4.93E-04	9.55E-04	1.20E-04	7.18E-04	1.16E-04	5.46E-04	M25
3.44E-04	2.87E-04	4.72E-04	2.83E-04	2.87E-04	-	6.60E-04	1.52E-04	2.17E-04	3.45E-04	9.57E-04	1.17E-04	4.92E-04	1.08E-04	5.01E-04	M26
3.46E-04	4.51E-04	5.83E-04	3.18E-04	6.29E-04	-	4.10E-04	2.27E-04	2.21E-04	2.88E-04	9.61E-04	9.01E-05	5.34E-04	4.84E-05	3.88E-04	M27
6.67E-04	6.12E-04	7.07E-04	4.15E-04	9.28E-04	-	3.78E-04	4.47E-04	4.02E-04	4.24E-04	8.86E-04	1.07E-04	5.34E-04	1.20E-04	4.54E-04	M28
7.62E-04	8.75E-04	7.46E-04	7.43E-04	1.00E-03	-	9.45E-04	6.75E-04	5.05E-04	5.97E-04	8.86E-04	3.40E-04	5.93E-04	4.27E-04	4.65E-04	M29
9.96E-04	7.52E-04	7.31E-04	6.85E-04	7.95E-04	-	1.06E-03	9.42E-04	4.14E-04	1.14E-03	7.64E-04	4.41E-04	9.25E-04	3.48E-04	7.81E-04	M30
2.79E-04	6.03E-04	6.99E-04	6.92E-04	0.00E+00	-	8.33E-04	1.59E-04	2.30E-04	6.84E-04	8.74E-04	1.31E-04	6.91E-04	1.17E-04	7.07E-04	M31
3.28E-04	1.66E-04	3.28E-04	2.48E-04	2.61E-04	-	4.90E-04	1.41E-04	2.31E-04	4.76E-04	1.17E-03	9.99E-05	6.38E-04	1.15E-04	6.39E-04	M32
3.95E-04	3.57E-04	5.19E-04	2.96E-04	6.68E-04	-	8.33E-04	2.28E-04	2.80E-04	3.43E-04	1.18E-03	1.12E-04	6.33E-04	9.20E-05	5.44E-04	M33
8.11E-04	6.22E-04	7.50E-04	5.25E-04	1.08E-03	-	4.90E-04	5.29E-04	6.71E-04	3.81E-04	1.19E-03	1.54E-04	6.34E-04	1.36E-04	5.41E-04	M34
1.07E-03	1.28E-03	9.56E-04	9.52E-04	1.56E-03	-	2.39E-04	6.31E-04	8.93E-04	5.90E-04	1.04E-03	2.51E-04	1.00E-03	4.72E-04	5.35E-04	M35
1.46E-03	1.27E-03	2.56E-04	1.04E-03	1.10E-03	-	7.02E-04	1.26E-03	5.78E-04	1.55E-03	1.44E-03	5.97E-04	4.86E-04	4.22E-04	8.58E-04	M36
2.33E-04	7.86E-04	9.15E-04	9.06E-04	0.00E+00	1.35E-03	1.19E-03	1.64E-04	3.00E-04	8.98E-04	1.25E-03	1.65E-04	7.73E-04	1.64E-04	9.43E-04	M37
2.56E-04	1.97E-04	2.12E-04	2.08E-04	2.08E-04	1.45E-03	1.32E-03	1.97E-04	2.08E-04	6.40E-04	1.36E-03	1.14E-04	7.87E-04	1.36E-04	7.81E-04	M38
5.33E-04	3.47E-04	4.66E-04	3.80E-04	6.37E-04	1.12E-03	1.06E-03	3.26E-04	2.53E-04	4.70E-04	1.50E-03	1.39E-04	7.78E-04	1.38E-04	7.30E-04	M39
1.07E-03	4.94E-04	8.03E-04	7.09E-04	1.17E-03	1.17E-03	6.05E-04	6.76E-04	4.20E-04	5.29E-04	1.74E-03	1.51E-04	5.80E-04	3.05E-04	7.85E-04	M40
1.61E-03	1.34E-03	1.42E-03	1.37E-03	1.86E-03	6.11E-04	6.61E-04	5.12E-04	3.09E-04	1.43E-03	2.11E-03	2.29E-04	7.90E-04	6.86E-04	6.51E-04	M41
1.46E-03	1.68E-03	1.70E-03	1.41E-03	3.21E-03	1.61E-03	1.57E-03	1.17E-03	6.29E-03	1.87E-03	3.02E-03	2.29E-04	1.14E-03	8.19E-04	2.23E-03	M42

Table 4: Normalized maximum amplitude of the responses corresponding to the deleted members in nonlinear dynamic analysis.

num M	U4	U3	U2	U1	L3	L2	L1	S4	S3	S2	S1	B4	B3	B2	B1	avg row	num M
M1	22%	43%	21%	30%	0%	-	15%	21%	31%	23%	57%	11%	13%	21%	23%	24%	M1
M2	16%	25%	16%	20%	17%	-	13%	9%	12%	12%	49%	6%	13%	12%	32%	18%	M2
M3	16%	12%	19%	13%	7%	-	10%	8%	10%	12%	31%	1%	9%	13%	8%	12%	M3
M4	16%	10%	6%	8%	9%	-	9%	6%	5%	9%	22%	2%	6%	13%	5%	9%	M4
M5	17%	9%	17%	7%	11%	-	10%	5%	3%	8%	14%	3%	5%	13%	7%	9%	M5
M6	15%	7%	13%	7%	12%	-	8%	4%	3%	11%	12%	4%	6%	10%	5%	8%	M6
M7	16%	17%	20%	19%	0%	-	10%	7%	15%	20%	8%	4%	3%	13%	22%	13%	M7
M8	10%	9%	23%	14%	8%	-	5%	10%	10%	17%	12%	4%	9%	4%	9%	10%	M8
M9	9%	8%	10%	10%	6%	-	4%	6%	7%	12%	10%	3%	7%	3%	10%	7%	M9
M10	6%	8%	10%	9%	7%	-	3%	6%	8%	9%	9%	2%	5%	3%	7%	7%	M10
M11	4%	8%	10%	6%	7%	-	2%	6%	7%	7%	8%	2%	6%	2%	6%	6%	M11
M12	5%	7%	8%	4%	6%	-	4%	9%	6%	10%	9%	4%	8%	2%	7%	6%	M12
M13	9%	10%	11%	10%	0%	-	7%	4%	10%	9%	13%	3%	6%	2%	11%	7%	M13
M14	8%	8%	13%	7%	5%	-	7%	5%	4%	8%	9%	2%	8%	4%	4%	7%	M14
M15	8%	8%	10%	9%	7%	-	6%	3%	6%	8%	7%	1%	7%	3%	7%	6%	M15
M16	7%	9%	10%	8%	10%	-	4%	5%	7%	8%	7%	2%	6%	3%	6%	7%	M16
M17	6%	9%	10%	7%	9%	-	3%	6%	6%	12%	9%	4%	8%	3%	6%	7%	M17
M18	7%	7%	9%	5%	8%	-	3%	8%	4%	8%	11%	4%	9%	3%	9%	7%	M18
M19	7%	7%	8%	8%	0%	-	7%	5%	7%	4%	14%	2%	8%	2%	9%	6%	M19
M20	5%	7%	9%	5%	5%	-	9%	2%	4%	20%	11%	2%	6%	1%	6%	7%	M20
M21	7%	8%	10%	5%	9%	-	8%	3%	5%	5%	11%	1%	7%	1%	5%	6%	M21
M22	8%	9%	11%	7%	12%	-	6%	4%	7%	6%	10%	1%	8%	3%	6%	7%	M22
M23	9%	10%	10%	8%	12%	-	4%	8%	6%	9%	11%	5%	9%	4%	7%	8%	M23
M24	11%	9%	9%	8%	11%	-	11%	10%	4%	15%	12%	5%	11%	4%	11%	9%	M24
M25	6%	6%	8%	8%	0%	-	13%	4%	5%	8%	15%	2%	11%	2%	9%	7%	M25
M26	5%	5%	7%	4%	5%	-	10%	2%	3%	5%	15%	2%	8%	2%	8%	6%	M26
M27	5%	7%	9%	5%	10%	-	7%	4%	4%	5%	15%	1%	8%	1%	6%	6%	M27
M28	11%	10%	11%	7%	15%	-	6%	7%	6%	7%	14%	2%	8%	2%	7%	8%	M28
M29	12%	14%	12%	12%	16%	-	15%	11%	8%	9%	14%	5%	9%	7%	7%	11%	M29
M30	16%	12%	12%	11%	13%	-	17%	15%	7%	18%	12%	7%	15%	6%	12%	12%	M30
M31	4%	10%	11%	11%	0%	-	13%	3%	4%	11%	14%	2%	11%	2%	11%	8%	M31
M32	5%	3%	5%	4%	4%	-	8%	2%	4%	8%	19%	2%	10%	2%	10%	6%	M32
M33	6%	6%	8%	5%	11%	-	13%	4%	4%	5%	19%	2%	10%	1%	9%	7%	M33
M34	13%	10%	12%	8%	17%	-	8%	8%	11%	6%	19%	2%	10%	2%	9%	10%	M34
M35	17%	20%	15%	15%	25%	-	4%	10%	14%	9%	16%	4%	16%	8%	8%	13%	M35
M36	23%	20%	4%	16%	17%	-	11%	20%	9%	25%	23%	9%	8%	7%	14%	15%	M36
M37	4%	12%	15%	14%	0%	21%	19%	3%	5%	14%	20%	3%	12%	3%	15%	11%	M37
M38	4%	3%	3%	3%	3%	23%	21%	3%	3%	10%	22%	2%	13%	2%	12%	9%	M38
M39	8%	6%	7%	6%	10%	18%	17%	5%	4%	7%	24%	2%	12%	2%	12%	9%	M39
M40	17%	8%	13%	11%	19%	19%	10%	11%	7%	8%	28%	2%	9%	5%	12%	12%	M40
M41	26%	21%	23%	22%	30%	10%	10%	8%	5%	23%	34%	4%	13%	11%	10%	17%	M41

M42	23%	27%	27%	22%	51%	26%	25%	19%	100%	30%	13%	48%	18%	13%	35%	32%	M42
	10.7%	11.0%	11.8%	10.0%	10.1%	19.4%	9.4%	7.1%	9.3%	11.3%	16.7%	4.3%	9.2%	5.2%	10.4%	avg clmn	
		43.5%				38.9%				44.4%				29.1%		sum U,L, B,S	

14) The red text indicates the analysis, in which local instability has occurred in the members of the boundary modules; and to avoid halting the analysis by the software, only the load of the boundary node members (and not its members) attached to the desired member is removed.

15) Among the boundary modules, the M1 module contains most of the cases discussed in the previous paragraph. Since this module is a type of boundary modules along the barrel vault length and span, it is the most critical module in terms of creating local instability in the barrel vault. From M2 to M6, local instability occurs only once in the M4 module, which leads to node load removal. In other boundary modules of the longitudinal direction of the barrel vault, such as M7, M13, M19, M25, M31 ,and M37, the above load has occurred 2, 2, 2, 3, 2 times, and once, respectively. Accordingly, the M1 module is the most critical module due to local instability. Boundary modules along the barrel vault span are not sensitive except in one case. Among the fifteen members of each of the boundary modules of the longitudinal direction of the barrel vault, there is a possibility of local instability in some of their members (a maximum of four cases).

16) In comparing the sensitivity of different types of boundary modules (along the barrel vault length and span), the B members are not sensitive to local instability except in one case. S members, except S2 members, are not sensitive; the L members are not sensitive, and the U members are not sensitive in the U3 member, but local instability is possible in members U1, U2, and U4. In other words, the analysis related to the removal of S2 members in all boundary modules along the longitudinal direction of the span leads to local instability. Therefore, it is the most critical one related to the mentioned case. Also, in other members of the structure except members B2, U1, U2, and U4, the studied structure is not sensitive to local instability.

17) The member L3 of the M38 module has been previously introduced by Ghandi and Habibi [17] as one of the members with maximum stress. According to Table 4, maximum stress alone does not indicate more damage than other members of the structure. Despite the existence of members with maximum stress, removing other members (with less stress) shows more unstable behavior.

18) Except for the analysis of the L3 member, removing members with maximum stress range leads to a greater oscillation amplitude than in other cases.

The last two rows in Table 4 represent the mean displacement corresponding to the removal of each type of module members (the average of each column of the table numbers) and the sum of the average displacements of B, S, L, and U members, respectively. According to these rows of Table 4, the maximum mean displacement is related to the S1 and L2 members. Moreover, the minimum mean displacements are related to the B4 and B2 members. In general, the maximum displacement is related to S and U members, and the minimum is related to B members. It can be stated that S members have critical behavior and B members have more stable behavior in the dynamic and nonlinear alternative path analysis of the tensegrity barrel vault.

Table 5 shows the number of analyses that led to the initial instability in the various members of the tensegrity barrel vault. The first row of the table shows the number of instabilities of each type of member, and the second row shows their sum. As shown in Table 5, U2 and U4 members have the maximum number of analyses leading to initial instability, while B1 and L3 members have the minimum number. In general, U and S are members with the maximum number of initial instabilities in their analysis, and L members have a stable behavior, and the minimum number of instabilities occurs in the analysis of these members. According to (Table 5) it can be stated that U and S members have critical behavior, and L members show stable behavior in the analysis of the dynamic and nonlinear alternative path analysis of tensegrity barrel vault.

Table 6 shows the number of cases that the displacement of the structure during the analysis was reduced (green background in Table 4). According to Table 6, U2 and L1 members have the maximum number, and B1, B3, S1, S3, S2 and L3 members have the minimum number. In general, the U members have the highest number, and S and B members have the lowest number of reduced displacement analyses. Considering Table 4, from module M16 onwards, a green background is observed in most analyses of U2, U3, and U4 members. Therefore, if the reduction of the displacement of the structure is considered as the desired phenomenon at the time of removing the member, the behavior of the U members is more favorable, and the behavior of the S and B members is more unfavorable than the other members of tensegrity the barrel vault in the dynamic and nonlinear alternative path analysis.

Table 5: Number of instabilities of different module members in nonlinear dynamic alternative path analysis.

	U4	U3	U2	U1	L3	L2	L1	S4	S3	S2	S1	B4	B3	B2	B1
AVERAGE	8	4	8	5	2	3	4	5	6	5	6	4	6	5	1
SUM U,L,B,S		25				9				22				16	

Table 6: Number of analyses leading to reduced displacement at the time of removing the different members.

	U4	U3	U2	U1	L3	L2	L1	S4	S3	S2	S1	B4	B3	B2	B1
NUM	19	20	22	13	0	4	22	11	1	2	1	10	0	7	0
SUM U,L,B,S		74				26				15				17	

5. Conclusions

This paper describes the results of the numerical investigation performed the progressive collapse behavior of two-layer tensegrity barrel vaults. The aim of the current study was to the identification of critical members by performing a nonlinear dynamic analysis. For this purpose, members with different types and positions were suddenly removed from the structure one by one, and the behavior of the structure after removing the desired member was evaluated by performing nonlinear dynamic analysis in Abaqus finite element software. The results of the analysis performed in this article are as follows.

• No collapse was observed in any dynamic and nonlinear alternative path analyses.

• In general, the modules that are farther away from the center of the structure in the longitudinal direction of the barrel vault, the steady state prevails than the other modules.

• In the performed analysis, the modules that are closer to the center of the structure in the longitudinal direction of the barrel vault, show more critical behavior than the other modules.

• Members with maximum stress are not among the most critical members and their dynamic nonlinear alternative path analysis under the conditions of this study does not lead to the total or local collapse of the structure.

• The boundary nature of the removed member alone cannot lead to instability in the tensegrity barrel vault.

• In general, as the examined member is closer to the center of the barrel vault, the behavior of the member becomes more critical.

• In terms of maximum displacement, the removal of the compression members leads to the most displacement in the structure, and also in this case, the tensile members in the middle layer have the least value.

• Dynamic alternative path analyses of compression members show more critical behavior than the other members, while tensile members in the lower layer show more stable behavior.

• If reducing the structure displacement during the analysis of the present study is considered a desirable phenomenon, upper layer tensile members have a favorable behavior with the highest number of reductions in the conducted analysis.

Conflicts of interest

The authors declare that there is no conflict of interest.

References:

[1] Zhang, J., & Ohsaki, M. (2015). Tensegrity Structures. New York: Springer.

[2] Abedi, K., & Shekastehband, B. (2008). Static Stability Behaviour of Plane Double-Layer Tensegrity Structures. International Journal of Space Structures, 23(2), 89-102.

[3] Hanaor, A. (1991). Double-layer Tensegrity Grids: Static Load Response. II: Experimental Study. Journal of Structural Engineering, 1675–84.

[4] Xu, Y., Zhang, X., & Han, Q. (2021). Research on the Progressive Collapse Resistance of Single-Layer

Cylindrical Latticed Shells with AH Joints. Thin-Walled Structures, 158, Article 107178.

[5] El-Sheikh, A. (1997). Sensitivity of Space Trusses to Sudden Member Loss. International Journal of Space Structures, 12(1), 31-41.

[6] Murtha-Smith, E. (1988). Alternate Path Analysis of Space Trusses for Progressive Collapse. Journal of Structural Engineering, 114(9), 1978-1999.

[7] Shekastehband, B., Abedi, K., & Chenaghlou, M. R. (2011). Sensitivity Analysis of Tensegrity Systems Due to Member Loss. Journal of Constructional Steel Research, 67(9), 1325-1340.

[8] Shekastehband, B., & Abedi, K. (2013). Collapse Behavior of Tensegrity Systems Due to Cable Rupture. International Journal of Structural Stability and Dynamics, 13(05), Article 1250079.

[9] Shekastehband, B., Abedi, K., Dianat, N., & Chenaghlou, M. R. (2012). Experimental and Numerical Studies on the Collapse Behavior of Tensegrity Systems Considering Cable Rupture and Strut Collapse with Snap-Through. International Journal of Non-Linear Mechanics, 47(7), 751-768.

[10] Shekastehband, B., Abedi, K., & Dianat, N. (2014). Experimental and Numerical Studies on the Progressive Collapse Behavior of Tensegrity Systems. International journal of space structures, 29(1), 9-24.

[11] Al Sabouni-Zawadzka, A., & Gilewski, W. (2014). Control of Tensegrity Plate Due to Member Loss. Procedia Engineering, 91, 204-209.

[12] Shekastehband, B. (2017). Collapse Mechanisms of Single Curvature Tensegrity Systems. International Journal of Steel Structures, 17(3), 1115-1129.

[13] Fu, F., & Parke, G. A. R. (2018). Assessment of the Progressive Collapse Resistance of Double-Layer Grid Space Structures Using Implicit and Explicit Methods. International Journal of Steel Structures, 18(3), 831-842.

[14] Sychterz, A. C., & Smith, I. F. (2018). Using Dynamic Measurements to Detect and Locate Ruptured Cables on a Tensegrity Structure. Engineering Structures, 173, 631-642.

[15] Shekastehband, B., & Ayoubi, M. (2019). Nonlinear Dynamic Instability Behavior of Tensegrity Grids Subjected to Impulsive Loads. Thin-Walled Structures, 136, 1-15.

[16] Yan, S., Zhao, X., Rasmussen, K. J., & Zhang, H. (2019). Identification of Critical Members for Progressive Collapse Analysis of Single-Layer Latticed Domes. Engineering Structures, 188, 111-120.

[17] Habibi Sheykh Ahmad, V., & Ghandi, E. (2019). Investigation of The Progressive Collapse of Double-Layer Tensegrity Barrel Vaults Composed of Square Simplexes with Finite Element Method. M.Sc. Thesis. University of Mohaghegh Ardabili.

[18] Mirzaaghazadeh, K., Abedi, K., & Shekastehband, B. (2020). Collapse Behavior of Tensegrity Barrel-Vault Structures Based on Di-Pyramid (DP) Units. International Journal of Structural Stability and Dynamics, 20(11), Article 2050119.

[19] Kahla, N. B., Ouni, M. H. E., Ali, N. B. H., & Khan, R. A. (2020). Nonlinear Dynamic Response and Stability Analysis of a Tensegrity Bridge to Selected Cable Rupture. Latin American Journal of Solids and Structures, 17.

[20] Wu, J., Zhang, L., He, Z., & Yan, Z. (2020). Comparative Analysis of Two Tensegrity Grids Considering Slack and Rupture of Cables. AIAA Journal, 58(5), 2321-2329.

[21] Nooshin, H., & Disney, P. (2000). Formex Configuration Processing I, International Journal of Space Structures, 15, 1–52.

[22] ABAQUS -Theory Manual. (1995). Hibbit, Karlsson, & Sorensen Inc., Providence, Rhode Island, USA.

[23] Tatemichi, I., Hatato, T., Anma, Y., & Fujiwara, S. (1997). Vibration Tests on a Full-Size Suspen-Dome Structure. International Journal of Space Structures, 12(3-4), 217-224.

[24] Bathe, K.J. (1996). Finite Element Procedures. Hoboken: Prentice Hall.

[25] Quirant, J., Kazi-Aoual, M.N., & Motro, R. (2003). Designing Tensegrity Systems: The Case of a Double Layer Grid. Engineering Structures, 25(1), 121–130.